

The Wake Dynamics of a Cylinder Moving Along a Plane Wall With Rotation and Translation

Bronwyn STEWART^{†*}, Kerry HOURIGAN[†], Mark THOMPSON[†] and
Thomas LEWEKE^{*}

[†]*Fluids Laboratory for Aeronautical and Industrial Research (FLAIR),
Department of Mechanical Engineering, Monash University, Clayton, 3800, Australia.*

^{*}*Institut de Recherche sur les Phénomènes Hors Equilibre,
CNRS/Universités Aix-Marseille, Technopôle de Château-Gombert,
49 rue Frédéric Joliot-Curie, BP 146, F-13384 Marseille Cedex, France.*

Abstract. A numerical investigation examined the 2-dimensional flow structures forming around a cylinder moving along a wall with different combinations of rolling and sliding, with Reynolds numbers, Re , ranging from 20 to 500. Past research has shown that both wall effects and rotation can suppress the mechanisms which bring about unsteady flow. Knowing this, it is natural to question how the flow will be affected when both these properties are present, as is the case for the cylinder rolling along a wall. Results indicate that the transition from steady to time-varying flow is strongly influenced by the rate of rotation of the body, and for the case of reversed rolling, the onset of unsteady flow is delayed until Reynolds numbers above 400.

Key words: wake dynamics, flow control, rolling cylinder.

1. Introduction

The current study utilised a two-dimensional, spectral element method to examine the flows occurring around a cylinder moving along a wall with several different combinations of rolling and sliding. Past research has shown that the flow structures forming around a stationary cylinder change dramatically when the body is in close proximity to a wall, and vortex shedding may be suppressed [1, 2]. Furthermore, the unsteady flow around an isolated cylinder may be suppressed if the cylinder is rotating at a sufficient speed, relative to the free-stream velocity [3]. The rate of rotation at which vortex shedding is suppressed is a function of the Reynolds number, Re , and results in a fully attached boundary layer and the formation of closed streamlines around the body [4]. Knowing that both wall effects and rotation can suppress the mechanisms which bring about unsteady flow, it is natural to question how the flow will be affected when both these properties are present, as is the case for the cylinder rolling along the wall. This configuration has the potential to control the formation of flow structures which may enhance particle deposition and mixing in both biological and industrial flows.

The problem geometry is shown in Fig. 1. The rotation rate of the cylinder, α , is defined as the ratio of rotational to translational cylinder velocity. That is, $\alpha = \omega D/2U$, where ω is the angular rotation, D is the cylinder diameter and U is the

translational velocity of the cylinder. Simulations were carried out for $\alpha = 1, 0.5, 0, -0.5$ and -1 to include a range of ‘reversed’ rolling when ω is negative (opposite in direction to that shown in Fig. 1). The Reynolds number of the flow is based on the cylinder diameter and ranges from 20 to 500.

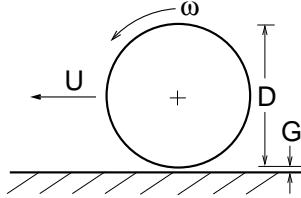


Figure 1. Problem configuration.

2. Wake dynamics behind the rolling and sliding cylinder

2.1. NUMERICAL METHOD AND RESOLUTION

The numerical code used a Galerkin method with seventh-order Lagrangian polynomials fitted to each macro-element of the mesh to solve for the relevant variables. A more complete description of the numerical method can be found in [5]. The mesh consisted of approximately 550 macro-elements, with dimensions of $100D$ to the upstream and downstream boundaries and $150D$ to the cross-stream boundary. This resulted in a blockage ratio of less than 1%. Further increases in polynomial order or domain size gave a variation in the Strouhal number and the mean lift and drag within 0.1% for $Re = 200$ and $\alpha = 1$.

To overcome numerical constraints, a small distance, G , was introduced between the cylinder and the wall. Increasing this distance from $0.004D$ to $0.01D$ allowed a small amount of fluid to pass between the body and the wall, however, the streamlines in the wake displayed no discernible change for $G < 0.01D$. $G = 0.005$ was used throughout the present study.

From this point forward, results are presented in the frame of reference attached to the cylinder centre, with the lower wall and the free-stream flow moving with the same velocity relative to the fixed, rotating cylinder.

2.2. STEADY FLOW

For each of the five cylinder rotation rates examined, the flow structures behind the body remain steady at the lower limit of Reynolds numbers studied ($Re = 20$). This flow is characterised by either 0, 1 or 2 closed areas of recirculating fluid. These recirculation regions are defined by the closed streamlines of the flow, and the upper and lower recirculation regions (labeled 1 and 2, respectively) are shown in Fig. 2. For cylinder motions with a positive rotation ($\alpha = 1, 0.5$) the upper recirculation region (1), is always present and encircling the body. This occurs as the cylinder motion entrains a fluid layer and moves it toward the contact region. The fluid being forced into the constriction then reverses direction and passes back over the top of the body. As the fluid moves downstream past the cylinder, it moves into the low pressure region behind the body where it is then sucked into the constriction at the rear of the body and re-entrained by the cylinder motion (see Fig. 2(a)).

When the cylinder is sliding along the wall with no rotation present (Fig. 2(b)), the topology of the flow is altered, and the upper recirculation region no longer encircles the cylinder. Instead, there exists points of flow separation and reattachment on the surface of the cylinder. The position of these separation and reattachment points remains relatively stable as Re is increased in the steady flow regime.

For both the sliding cylinder and the cylinder with positive rotation, streamlines near the wall only form a closed recirculation region, (2), when Re is increased beyond a critical value. For Re below this value a smaller region of upstream flow is observed but with no closed streamlines present.

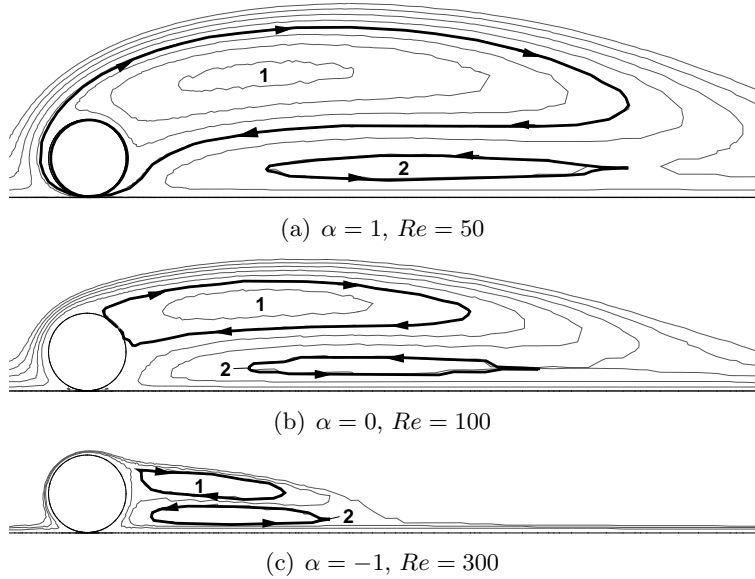


Figure 2. Upper and lower recirculation regions.

When the rotation of the cylinder has a negative value it is possible for the flow near the body and the wall to remain fully attached. When negative rotation is present, the flow entering the constriction near the wall is then able to reverse direction and be transported around the body in the cylinder boundary layer.

The increased flow attachment for negative α has a stabilising effect on the wake which prevents the formation of recirculation regions 1 and 2 for Reynolds number less than $Re \approx 70$ for $\alpha = -0.5$ and $Re \approx 115$ for $\alpha = -1$. When the upper recirculation region (1) is present, it no longer encircles the body but is instead separated from the cylinder by the attached boundary layer flow.

The effect of increasing Re and varying the rotation rate is shown below in Figs.3(a), 3(b) and 3(c). Increasing Re results in a near linear increase in the length of the steady recirculation zones. This is in agreement with observations of the steady flow around wall-mounted bodies and the backward facing step [6, 7].

As the rotation rate is varied between rolling (Fig. 3(a)), sliding (Fig. 3(b)) and reversed rolling (Fig. 3(c)), the wake narrows and moves closer to the wall. This is particularly apparent for the cases of reversed rotation. Another change in flow topology, which becomes apparent for negative α , is that associated with the formation of the upper and lower recirculation regions. For the cases of $\alpha = 1, 0.5, 0$ and -0.5 the upper recirculation region forms from the shear layer at lower Reynolds numbers, before recirculation region 2. However, as α becomes more negative, the

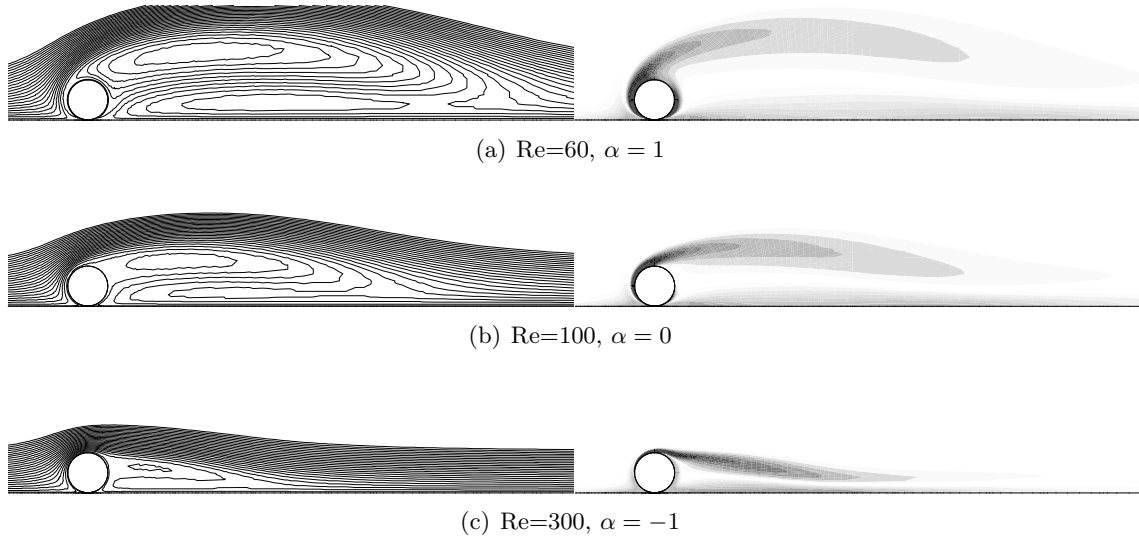


Figure 3. Streamlines and vorticity contours for steady flow.

recirculation region nearest the wall forms first. For $\alpha = -1$, even after appearance of recirculation region 1, the recirculating flow near the wall remains the larger of the two, which is not the case for the other values of α .

This difference in the relative size of the two areas of recirculating fluid is shown in Fig. 4 for the two cases of negative cylinder rotation studied. For increasing Re (until the limit of steady flow), the filled curves in Fig. 4 indicate the length of the recirculation zones measured from the upstream to downstream-most points. Zones 1 and 2 are as defined in Fig. 2 and x^* is the stream wise distance scaled by D . For $\alpha = -0.5$ the size of the two recirculation zones is comparable but with zone 1 occurring first, at lower Re . As described above, as α became more negative the formation of the recirculation regions was suppressed and there was a larger range of Re for which no closed regions of recirculating flow was observed.

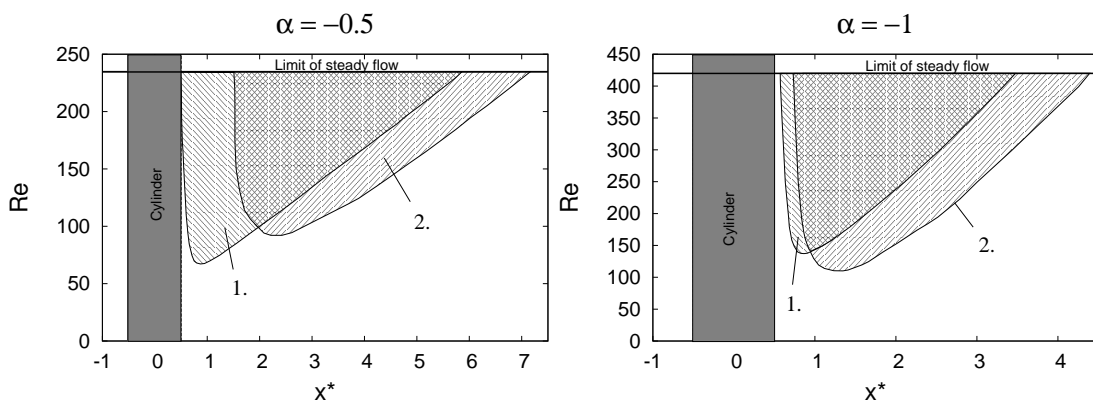


Figure 4. Filled curves indicate the regions in the x direction occupied by the two steady recirculation zones. For $\alpha = -0.5$ the upper recirculation region (1) appears at lower Re , while for $\alpha = -1$ the recirculation region nearest the wall (2) forms first.

During the steady flow regime the drag and lift forces on the body decrease smoothly according to a power law of the form $C_D \propto Re^{-b}$, where $0.74 < b < 0.80$. The results

for the drag coefficient at $\alpha = -1, 0$ and 1 are shown in Fig. 5.

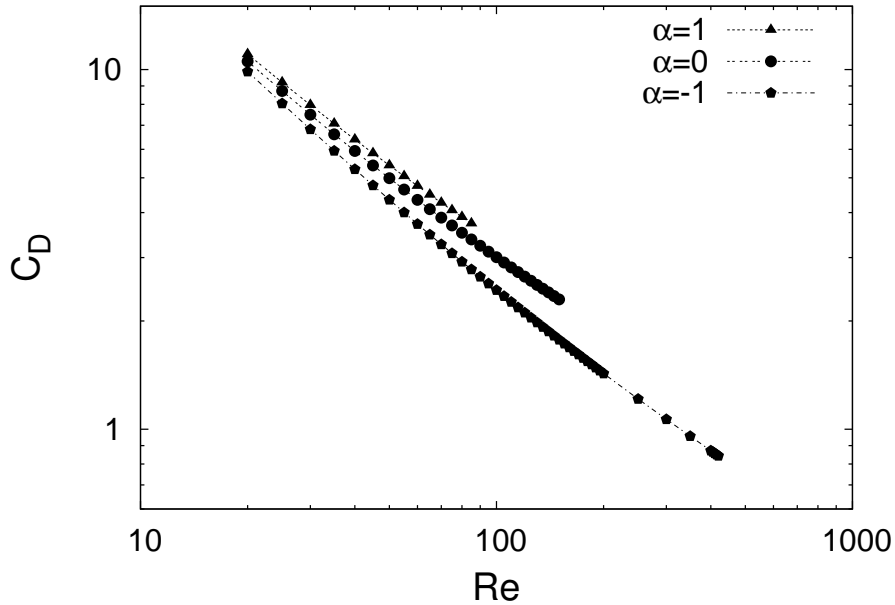


Figure 5. Coefficient of drag for varying Re and α .

As the rotation rate is varied the dominant force acting on the body changes from being a lift force at $\alpha = -1$ to a drag dominated system when the cylinder is sliding along the wall or moving with a positive rotation. This is shown in Fig. 6 for $Re = 80$. As the cylinder undergoes larger magnitude negative rates of rotation, the high pressures in the contact region and the lower pressures over the top of the body create a net lift force. In addition, the attached flow around the body acts to reduce the pressure drag.

2.3. UNSTEADY FLOW

For each of the five rotation rates under examination, the flow undergoes a transition from steady flow to periodic vortex shedding as Re increases. No hysteresis was observed for this transition and the critical Re dividing these two regimes is shown in Fig. 7. As described above for the development of the steady recirculation zones, negative values of α tend to enhance the stability of the flow, and for $\alpha = -1$ the flow does not undergo the transition to time-varying flow until $Re > 400$.

Once the flow becomes unsteady, the wake is characterised by vorticity from the upper shear layer inducing opposite-sign vorticity at the wall. These regions of opposite sign vorticity then move away from the wall and form a rotating vortex pair similar to those observed by Arnal *et al.* [8] for the square cylinder sliding along a wall. A typical shedding period is shown in Fig. 8 at $Re = 200$ for the sliding cylinder with $\alpha = 0$. The movement downstream of the shed vortex pair is observed (from top to bottom) with the next image in the sequence starting again from the top. A clockwise rotation of the vortex pair takes place due to the higher strength of the vortex which is shed from the cylinder shear layer.

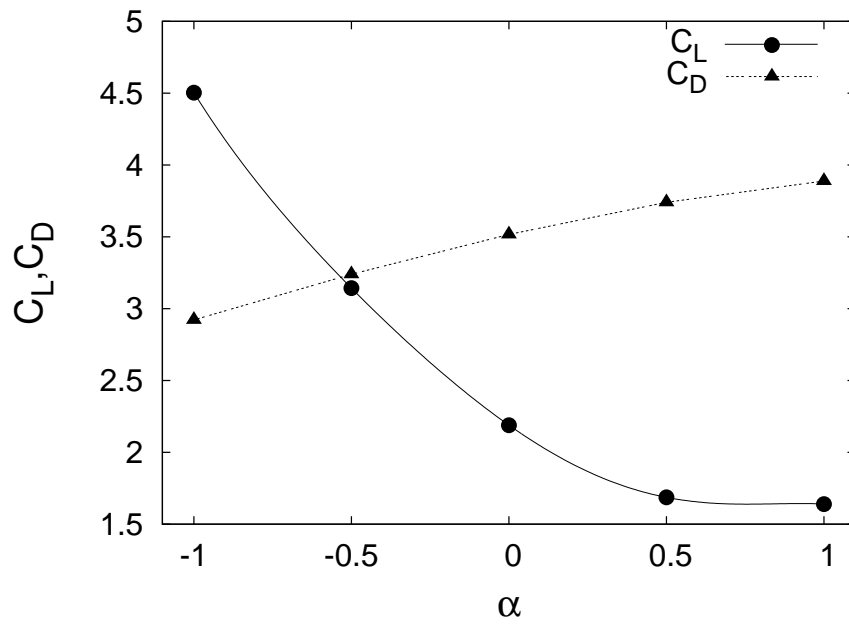


Figure 6. Coefficients of lift and drag for $Re = 80$.

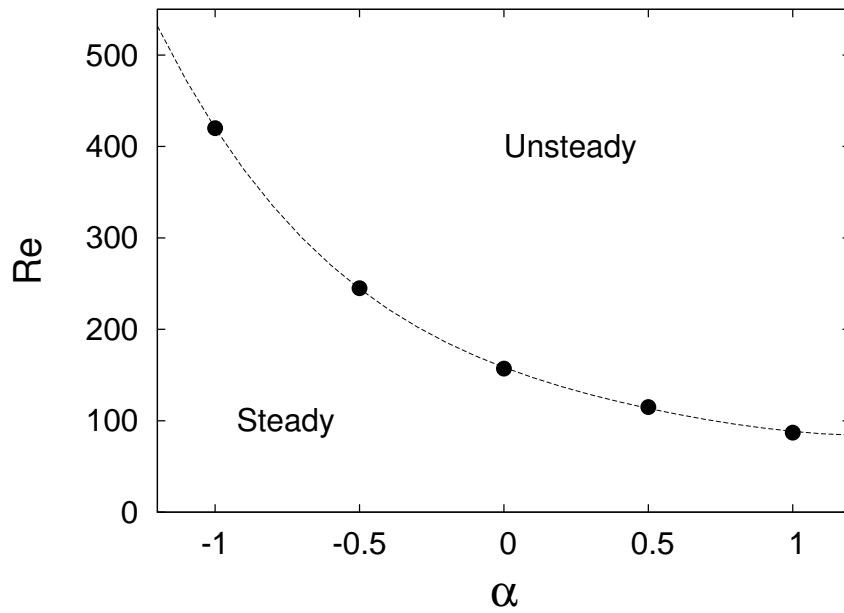


Figure 7. Transition from steady to unsteady flow for varying α .

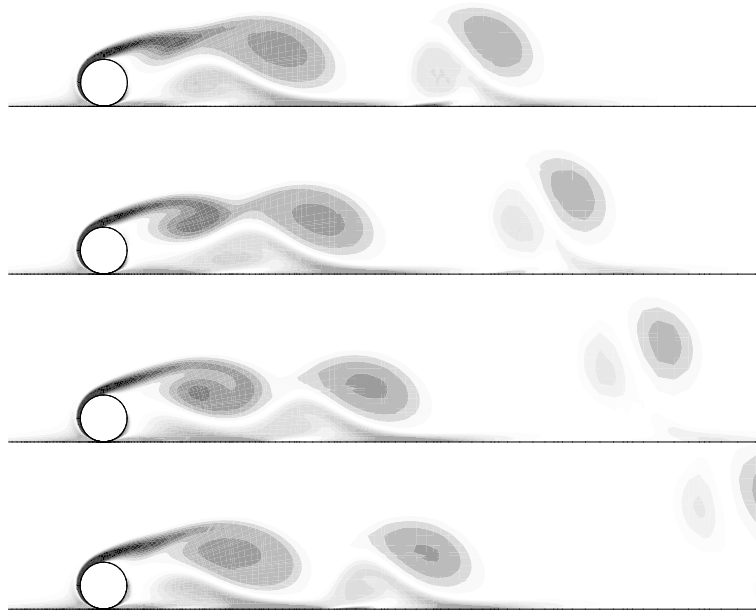


Figure 8. Vorticity contours for the cylinder with $\alpha = 0$ at $Re = 200$ over a single shedding cycle.

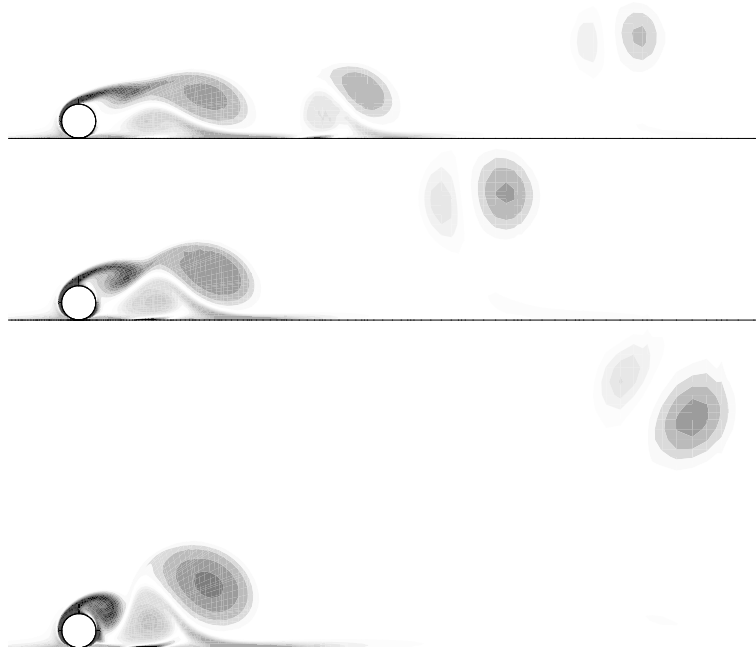


Figure 9. Vorticity contours for unsteady flow at $Re = 200$ for $\alpha = 0$, $\alpha = 0.5$ and $\alpha = 1$ (from top).

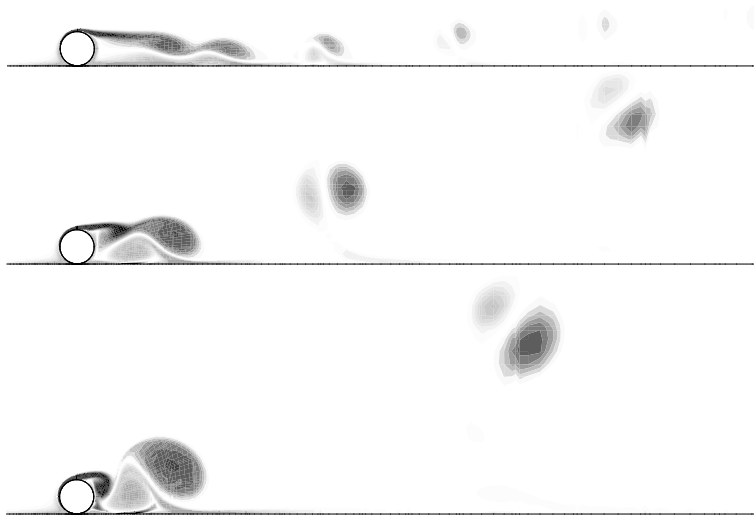


Figure 10. Vorticity contours for unsteady flow at $Re = 450$ for $\alpha = -1$, $\alpha = -0.5$ and $\alpha = 0$ (from top).

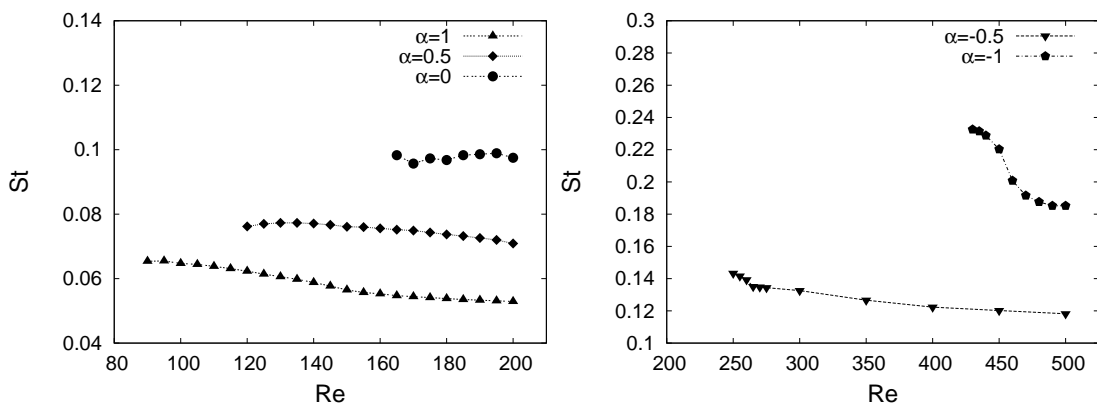


Figure 11. Variation of Strouhal number with cylinder rotation rate.

Increasing α from 0 to 1 at $Re = 200$ results in a considerably shorter formation length and reduces the frequency of vortex shedding. This can be seen in Fig. 9, which shows the three rotation rates at approximately the same moment in the shedding cycle (taken at the moment of maximum lift). The increasing spatial separation of the shed vortex pair is a reflection of the change in shedding frequency and Strouhal number, St . The strength of the shed vorticity also increases with the rotation rate, resulting in the shed vortex pair being propelled further from the wall. The same trends are observed in Fig. 10, as α is increased from negative rotation to sliding ($\alpha = 0$).

For each cylinder rotation the frequency of vortex shedding appeared to be largely insensitive to Re , with the exception of the case of $\alpha = -1$. These trends are shown in Fig. 11 and at $Re \approx 450$ the shedding in the reversed rolling case experiences a sudden decrease in the Strouhal number. However, from Fig. 10 it is observed that the strength of the shed vorticity is also much less and the vortex pairs have all but disappeared by a distance of $15D$ downstream. From these observations

it is apparent that the imposed rotation of the cylinder is capable of either delaying or enhancing the onset of unsteady flow, depending on the magnitude and direction of rotation.

3. Conclusions

When the cylinder has a negative imposed rotation as it moves along the wall the stability of the wake is enhanced and the wake region narrows and moves towards the wall. For $\alpha = -1$ the wake is highly stable, and the transition to unsteady flow is not reached until $Re \approx 420$. As the rotation rate is varied from reversed rolling to sliding ($\alpha = 0$), the steady wake region increases in both length and distance from the wall. At $Re = 200$, the sliding cylinder wake is unsteady and the flow is characterised by vorticity from the upper shear layer inducing opposite sign vorticity at the wall. These regions of opposite sign vorticity then move away from the wall and form a rotating vortex pair. Increasing α from 0 to 1 at constant Re results in a considerably shorter formation length and increases the strength of the shed vorticity in the wake. The frequency of vortex shedding appeared to be insensitive to the Reynolds number of the flow, except for the case of $\alpha = -1$ which experienced a rapid decrease in St at $Re \approx 450$.

Acknowledgments

This research was made possible via the financial support of an Australian Post-graduate Award.

References

- [1] C. Lei, L. Cheng, S. W. Armfield, and K. Kavanagh. Vortex shedding suppression for flow over a circular cylinder near a plane boundary. *Ocean Engineering*, 27:1109–1127, 2000.
- [2] A. Dipankar and T. K. Sengupta. Flow past a circular cylinder in the vicinity of a plane wall. *Journal of Fluids and Structures*, 20(3):403–423, April 2005.
- [3] S. Mittal and B. Kumar. Flow past a rotating cylinder. *Journal of Fluid Mechanics*, 476:303–334, 2003.
- [4] J. C. Padrino and D. D. Joseph. Numerical study of the steady-state uniform flow past a rotating cylinder. *Journal of Fluid Mechanics*, 557:191–223, 2006.
- [5] M. Thompson, K. Hourigan, and J. Sheridan. Three-dimensional instabilities in the wake of a circular cylinder. *Experimental Thermal and Fluid Science*, 12:190–196, 1996.
- [6] S. C. R. Dennis and Gau-Zu Chang. Numerical solutions for steady flow past a circular cylinder at Reynolds numbers up to 100. *Journal of Fluid Mechanics*, 42:471–489, 1970.
- [7] P. T. Williams and A. J. Baker. Numerical simulations of laminar flow over a 3D backward-facing step. *International Journal for Numerical Methods in Fluids*, 24:1159–1183, 1997.
- [8] M. P. Arnal, D. J. Goering, and J. A. C. Humphrey. Vortex shedding from a bluff body adjacent to a plane sliding wall. *Transactions of the American Society of Mechanical Engineers*, 113:384–398, 1991.